Electronic supplementary information

NEW CATALYSTS FOR THE ELECTROCHEMICAL REDUCTION OF PROTON

K. I. Utegenov,*[a] D. A. Valyaev,[b] T. T. Amatov,[c] A. Sournia-Saquet,[b]
O. V. Semeikin,[a] and N. A. Ustynyuk[a]

[a] *Nesmeyanov Institute of Organoelement Compounds, Russian Academy of Sciences,
ul. Vavilova 28, str. 1, Moscow, 119334 Russia*
[b] *LCC-CNRS, Université de Toulouse, CNRS,
205 route de Narbonne 31077 Toulouse cedex 4, France*
[c] *New York University Abu Dhabi, PO Box 129188, Saadiyat Island,
Abu Dhabi, United Arab Emirates*

Brief review of the state-of-the-art

The development of cheap catalysts for the electrochemical reduction of proton (ERP) to hydrogen, for example, as a source of energy storage, is of considerable interest. The word "cheap" in this context implies materials free of noble metals. The main attention in this research trend is given to the study of complexes imitating the structural motif of FeFe- and FeNi-hydrogenases [S1], as well as hydride [S2], phenanthroline [S3] and bipyridine complexes [S4]. The key steps in the proton reduction catalysis using these catalytic systems are the formation of M–H bonds and redox transformation of intermediate hydrides. At the same time, the formation of C–H bonds and their redox activation in the ERP catalysis cycles were reported for few examples [S5, S6]. In the present work, as is mentioned in the manuscript, we prepared and studied the complexes, the protonated forms of which contain a C–H bond conjugated with a multiple metal–carbon bond, and revealed their activity in the ERP.

General remarks

Cyclic voltammograms were recorded on an Autolab PGSTAT100 instrument controlled by the GPES 4.09 software in an argon atmosphere using a three-electrode cell consisting of a glassy carbon working electrode ($d = 3$ mm) and a platinum plate ($S = 1$ cm^2) as a counter electrode. The potentials were measured relative to saturated calomel electrode (SCE) and their values are given relative to the ferrocene/ferrocenium pair ($E = +0.46$ V in CH_2Cl_2 rel. SCE). For high scan rate experiments, a platinum working electrode ($d \approx 0.5$ mm) was used. The number of electrons $n(e)$ consumed was estimated comparing the observed peak heights with those of the one-electron Fc/Fc^+ or $(\eta^5\text{-}C_5Me_5)_2Fe/(\eta^5\text{-}C_5Me_5)_2Fe^+$ couples. All measurements were carried out in dry dichloromethane at the scan rate of 200 mV·s^{-1}; the concentration of the test compound was $1 \cdot 10^{-3}$ M. The supporting electrolyte was 0.1 M Bu_4NPF_6. The proton reduction experiments were carried out using $HBF_4 \cdot OEt_2$ (M = 161.93 g·mol^{-1}, d = 1.18 g·mL^{-1}) purchased from Sigma-Aldrich and diluted in dichloromethane, which was prepared diluting this acid (70 μL, 826 mg, 5.1 mmol) in 0.93 mL of dichloromethane. The cyclic voltammograms for **Re1** and **Fe1** are shown in Figs. S1 and S2 and the corresponding CVs recorded in the presence of acid are given in the manuscript as Figs. 1 and 2. The cyclic voltammograms for **Mn1** and **Mn2** are also given in Figs. S3–S8 for comparison. The cyclic voltammograms for **Mn3** and **Mn4** are shown in Figs. S9–S11. The values of the catalytic current in the proton reduction

experiments strongly depend on the quality of the electrode surface (the catalytic current obtained on the freshly polished electrode is two- to three-fold higher than that obtained upon repetitive scans); therefore, all cyclic voltammograms were recorded at least twice for better reproducibility.

The IR spectra of solutions were recorded in CaF_2 cells on Specord 75 IR and Specord M80 spectrophotometers (Carl Zeiss, Jena, Germany). The wavenumbers are given in cm^{-1} and the relative intensity is denoted by symbols s (strong), m (medium), or w (weak) in parentheses. The ^1H and ^{13}C NMR spectra were measured on Bruker AMX 300 and Bruker Avance II 600 instruments. The chemical shifts are referenced to the residual solvent signals (chloroform-d_1 or benzene-d_6).

Cyclic voltammograms
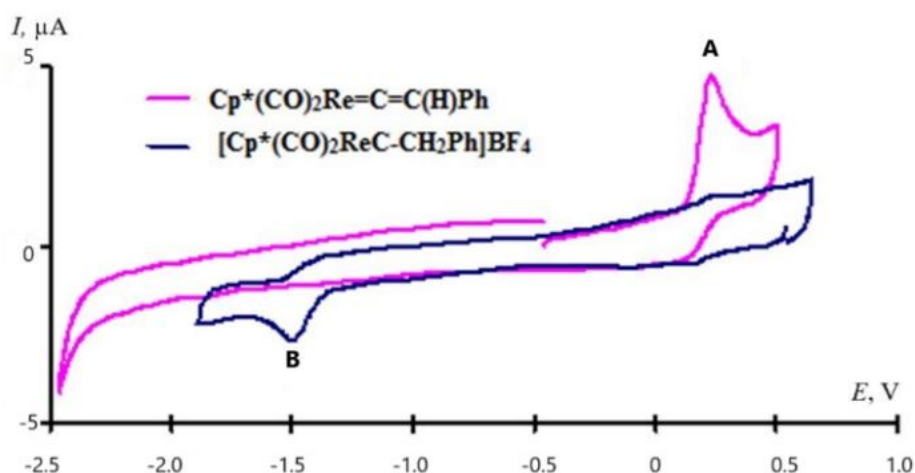
**Figure S1.** CV for $(\eta^5\text{-}C_5Me_5)(CO)_2Re=C=C(H)Ph$ (**Re1**) and its protonated form $(\eta^5\text{-}C_5Me_5)(CO)_2Re\equiv C\text{–}CH_2Ph$ (**Re1H$^+$**) (GC electrode, CH_2Cl_2, 0.1 M Bu_4NPF_6, $1\cdot10^{-3}$ M, 200 mV·s^{-1}, potentials are given relative to Fc/Fc$^+$).
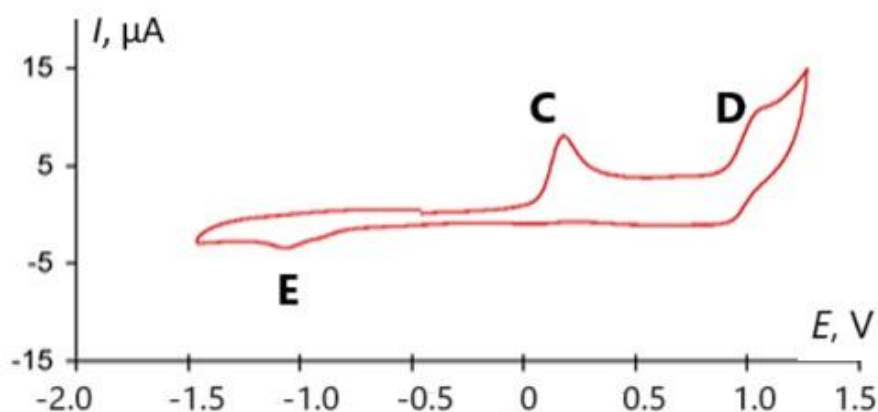
Figure S2. CV for $(\eta^5\text{-}C_5H_5)(CO)(Ph_3P)Fe\text{–}C\equiv C\text{–}Ph$ (**Fe1**) (GC electrode, CH_2Cl_2, 0.1 M Bu_4NPF_6, $1\cdot10^{-3}$ M, 200 mV·s^{-1}, potentials are given relative to Fc/Fc$^+$).

**Electrochemical data for earlier described compounds Mn1 and Mn2**

The electrochemical behavior of $(\eta^5\text{-}C_5H_5)(CO)(PPh_3)Mn=C=CHPh$ (**Mn1**) and its protonated form $[(\eta^5\text{-}C_5H_5)(CO)(PPh_3)Mn\equiv C\text{--}CH_2Ph]BF_4$ (**Mn1H$^+$**) in dichloromethane:
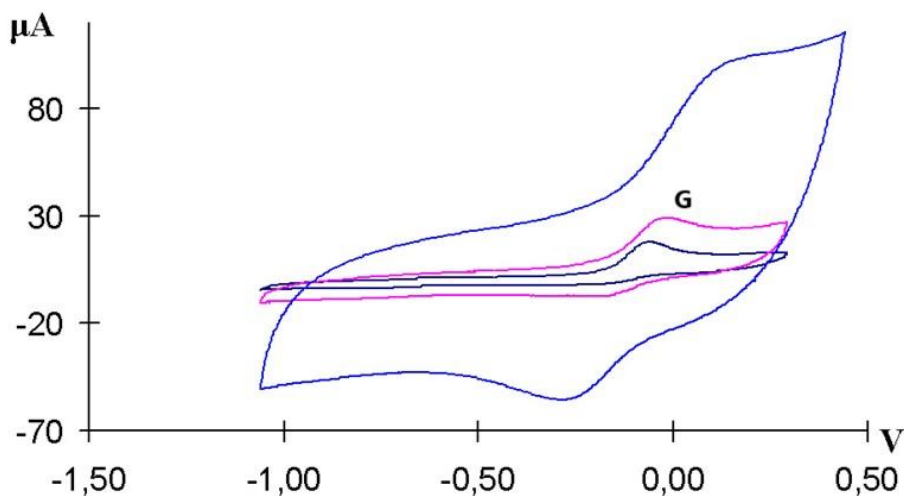
Figure S3. CVs for $(\eta^5\text{-}C_5H_5)(CO)(PPh_3)Mn=C=CHPh$ (**Mn1**) recorded at scan rates of 200 mV/s (black), 1 V/S (pink), and 10 V/s (blue) (GC electrode, CH_2Cl_2, 0.1 M Bu_4NPF_6, $1\cdot10^{-3}$ M, potentials are given relative to Fc/Fc$^+$).

The cyclic voltammogram of **Mn1** displays irreversible one-electron oxidation peak at 0.06 V (peak **G** in Fig. S3) on GC electrode at 200 mV/s. On the reverse scanning of potential, two peaks of the dimerization product were observed at –0.30 and –0.72 V. On the gold electrode at 200 mV/s, peak **G** is also irreversible one-electron with a potential value of –0.08 V, but no dimerization product peaks were observed on reverse scanning; therefore, the stability of the cationic species on glassy carbon is higher. With an increase in the scan rate, the oxidation peak **G** gradually becomes quasi-reversible: at a scan rate of 1 V/s, the reversibility is about 47% (ΔE = 130 mV) on GC electrode and, at a scan rate of 10 V/s (with ohmic drop 1000 Ohm), peak **G** becomes nearly reversible (95%) but with ΔE = 220 mV. On the gold electrode at a scan rate of 10 V/s, peak **G** showed 95% reversibility again with ΔE = 80 mV.
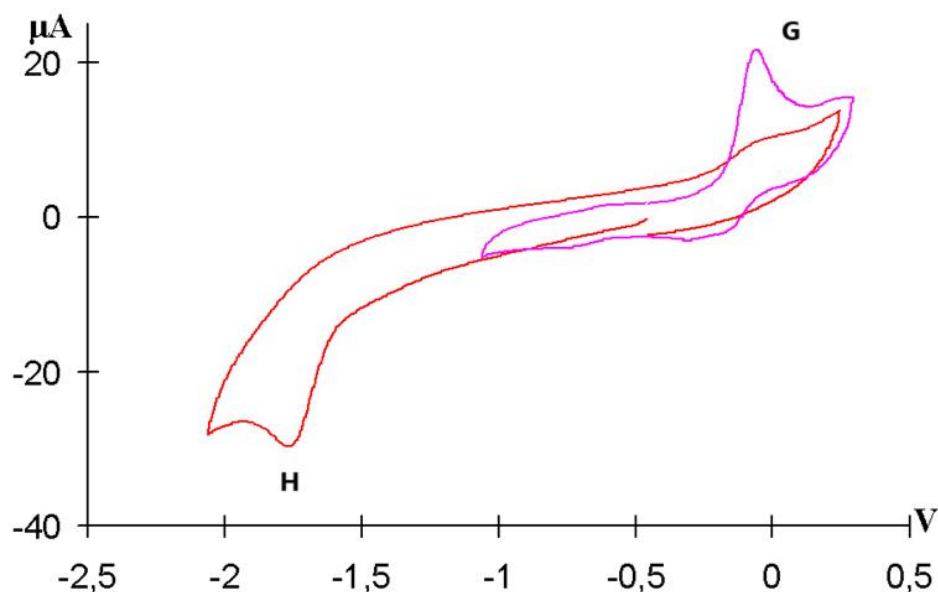
Figure S4. CVs for $[(\eta^5\text{-}C_5H_5)(CO)(PPh_3)Mn\equiv C\text{–}CH_2Ph]BF_4$ (**Mn1H**$^+$) recorded upon direct and reverse scans (GC electrode, CH_2Cl_2, 0.1 M Bu_4NPF_6, $1\cdot10^{-3}$ M, 200 mV/s, potentials are given relative to Fc/Fc$^+$).

The cyclic voltammogram of **Mn1H**$^+$ displays an irreversible one-electron reduction peak at –1.78 V (peak **H** in Fig. S4) on GC electrode at 200 mV/s. On the reverse scanning of potential, peak **G**, corresponding to the homolysis reaction product (η^5-$C_5H_5)(CO)(PPh_3)Mn=C=CHPh$ (**Mn1**), was observed at –0.06 V. On the gold electrode, the peak potential was lower than –1.66 V and no oxidation peak for $(\eta^5\text{-}C_5H_5)(CO)(PPh_3)Mn=C=CHPh$ was observed. The reduction peak for $[(\eta^5\text{-}C_5H_5)(CO)(PPh_3)Mn\equiv C\text{–}CH_2Ph]BF_4$ is completely irreversible even at 1000 V/s, showing very fast homolytic C_β–H bond cleavage process in 19e radical $\{(\eta^5\text{-}C_5H_5)(CO)(PPh_3)Mn^\bullet\equiv C\text{–}CH_2Ph\}$ (**Mn1H•**).

Electrochemical behavior of Mn1H$^+$ upon addition of HBF$_4$·OEt$_2$ in dichloromethane
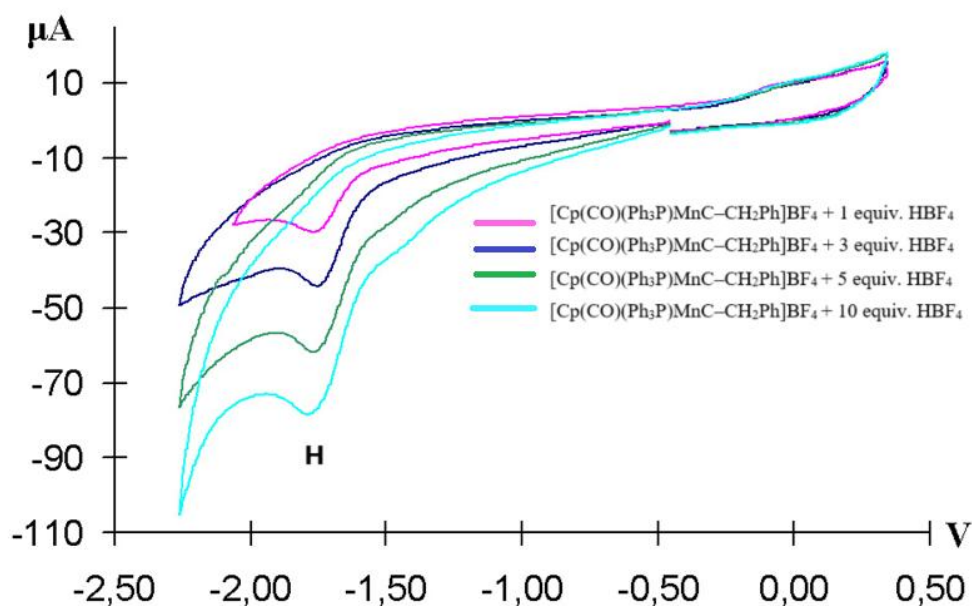
Figure S5. CVs for $[(\eta^5\text{-C}_5\text{H}_5)(CO)(PPh_3)Mn\equiv C\text{–}CH_2Ph]BF_4$ (**Mn1H$^+$**) recorded upon addition of different amounts of HBF$_4$ (GC electrode, CH$_2$Cl$_2$, 0.1 M Bu$_4$NPF$_6$, $1\cdot10^{-3}$ M, 200 mV/s, potentials are given relative to Fc/Fc$^+$).

Upon addition of HBF$_4$, the increasing catalytic current was observed and the peak potential gradually became more negative: –1.78 V for $[(\eta^5\text{-C}_5\text{H}_5)(CO)(PPh_3)Mn\equiv C\text{–}CH_2Ph]BF_4$ in solution, –1.81 V in the presence of 5 equiv. of HBF$_4$, and –1.86 V in the presence of 10 equiv. of HBF$_4$. In the presence of the acid, no oxidation peak of the corresponding vinylidene complex **Mn1** was observed due to its fast protonation.
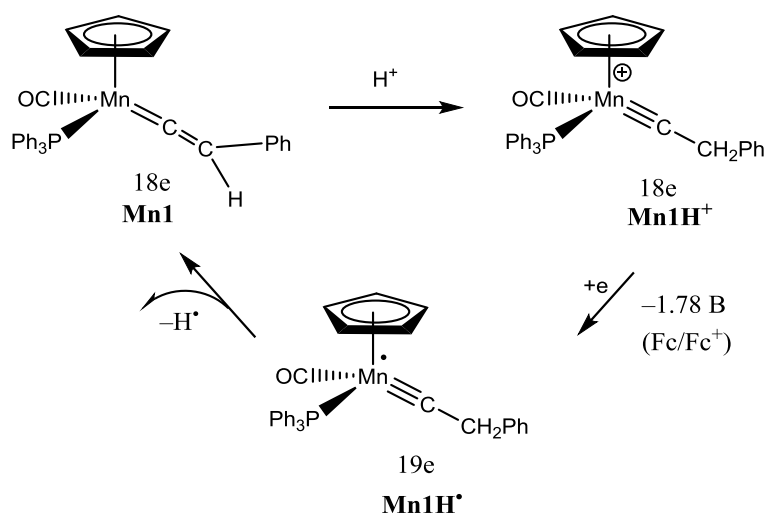

Scheme S2. Catalytic cycle for the electrochemical reduction of proton by complex **Mn2** in dichloromethane.

Electrochemical behavior of $(\eta^5\text{-}C_5H_5)(CO)_2Mn=C=C=CPh_2$ (Mn2) and its protonated form $[(\eta^5\text{-}C_5H_5)(CO)_2Mn\equiv C-CH=CPh_2]BF_4$ (Mn2H$^+$) in dichloromethane
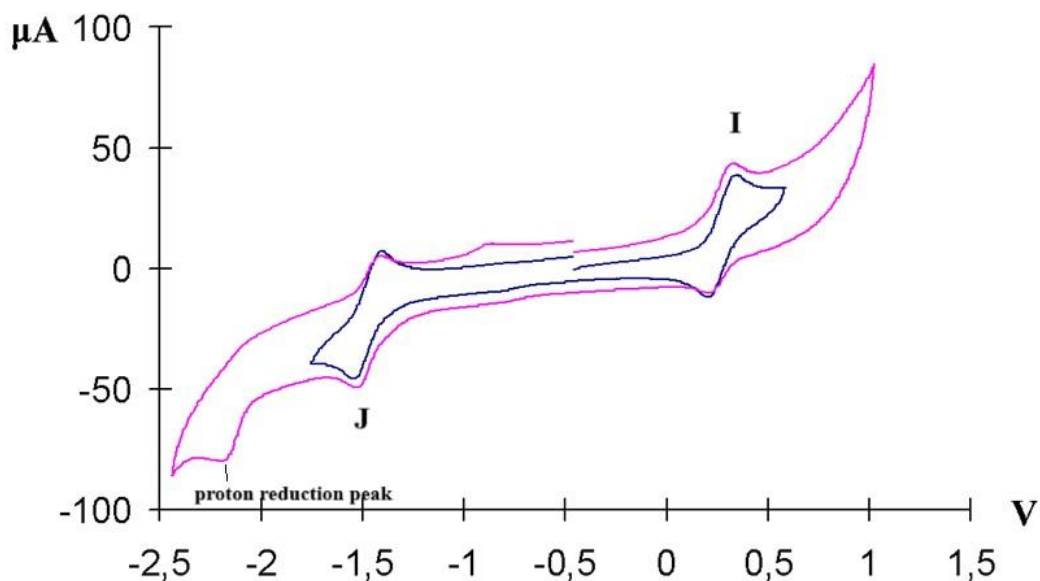
Figure S6. CV for $(\eta^5\text{-}C_5H_5)(CO)_2Mn=C=C=CPh_2$ (**Mn2**) (GC electrode, CH$_2$Cl$_2$, 0.1 M Bu$_4$NPF$_6$, $1\cdot10^{-3}$ M, 200 mV·s^{-1}, potentials are given relative to Fc/Fc$^+$).

The cyclic voltammogram of **Mn2** displays a reversible one-electron oxidation peak at +0.35 V (peak **I** in Fig. S6) on GC electrode at 200 mV/s ($\Delta E = 170$ mV). The second oxidation peak is irreversible at +1.19 V, on the reverse scanning of potential a reduction peak at –0.95 V (peak **J** in Fig. S6) corresponding to the cationic carbyne complex $[(\eta^5\text{-}C_5H_5)(CO)_2Mn^+\equiv C-CH=CPh_2]BF_4^-$ was observed, which is likely due to the proton abstraction from dichloromethane. The first reduction peak is reversible at –1.38 V and the second one is irreversible at –2.20 V. The second reduction peak that is observed in Fig. S6 seems to correspond to the reduction of proton itself.
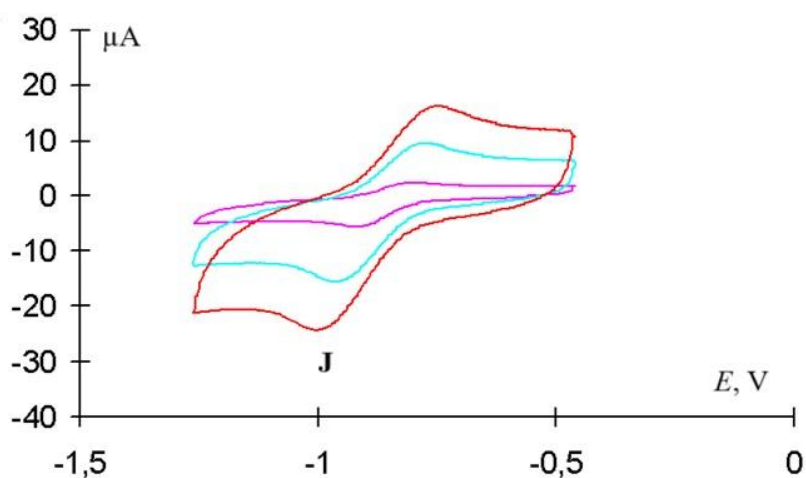
**Figure S7.** CV for $[(\eta^5\text{-}C_5H_5)(CO)_2Mn^+\equiv C-CH=CPh_2]BF_4^-$ (**Mn2H$^+$**) at scan rates of 10 mV/s (pink), 50 V/s (blue), and 100 V/s (red) (GC electrode, CH$_2$Cl$_2$, 0.1 M Bu$_4$NPF$_6$, $1\cdot10^{-3}$ M, potentials are given relative to Fc/Fc$^+$).

The cyclic voltammogram of **Mn2H⁺** displays an irreversible one-electron reduction peak at –0.93 V (peak **J** in Fig. S7) on GC electrode and –0.89 V on Pt electrode at a scan rate of 200 mV/s. At higher scan rates, peak **J** becomes quasi-reversible (the reversibility was 65% at 10 V/s, 77% at 50 V/s, and 96% at 100 V/s).

Electrochemical behavior of Mn2H$^+$ upon addition of HBF$_4$·OEt$_2$ in dichloromethane
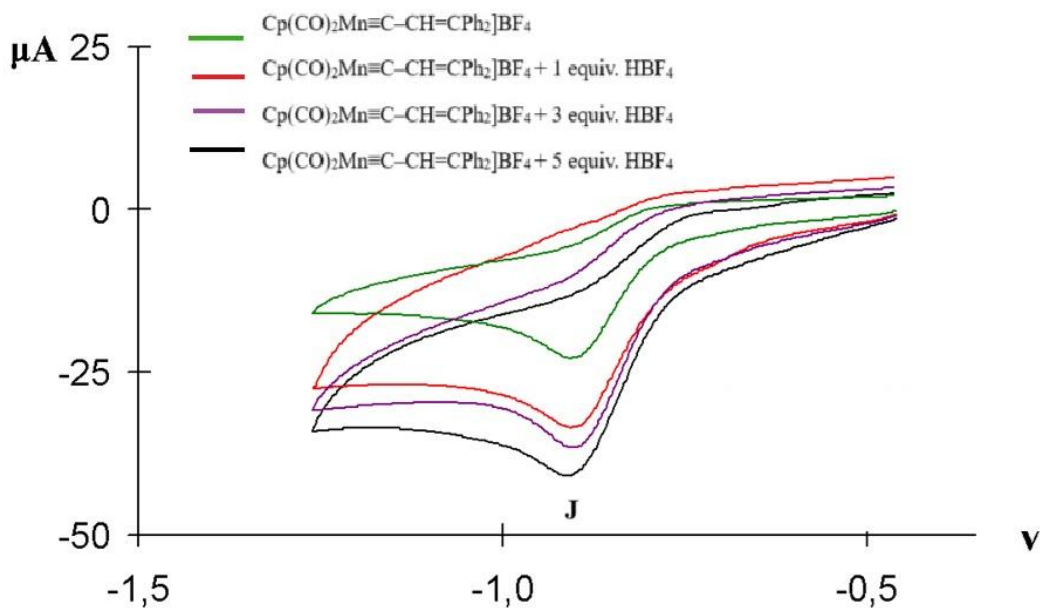
Figure S8. CVs for $[(\eta^5\text{-}C_5H_5)(CO)_2Mn\equiv C\text{–}CH_=CPh_2]BF_4$ (**Mn2H$^+$**) recorded upon addition of different amounts of HBF$_4$ (GC electrode, CH$_2$Cl$_2$, 0.1 M Bu$_4$NPF$_6$, 1×10^{-3} M, 200 mV/s, potentials are given relative to Fc/Fc$^+$).
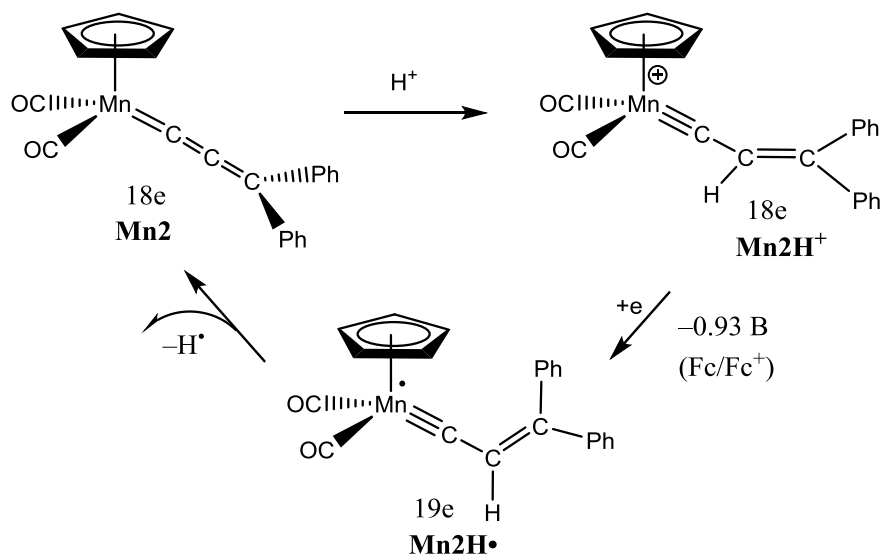
Scheme S2. Catalytic cycle for the electrochemical reduction of proton by complex **Mn2**.
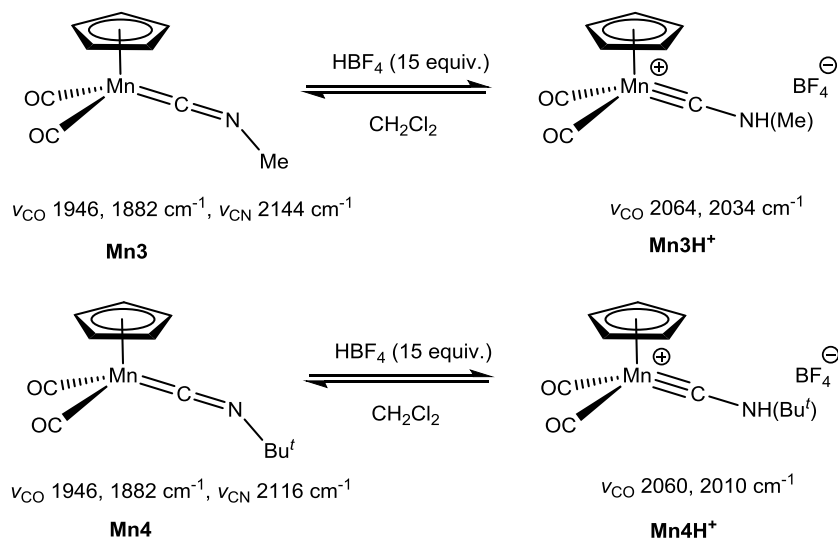
The above findings gave us impetus to extend the scope of this study to manganese isocyanides **Mn3** and **Mn4**, as it is mentioned in the manuscript. The electrocatalytic reduction of proton by complexes **Mn3** and **Mn4** was assumed to occur according to Scheme S3:
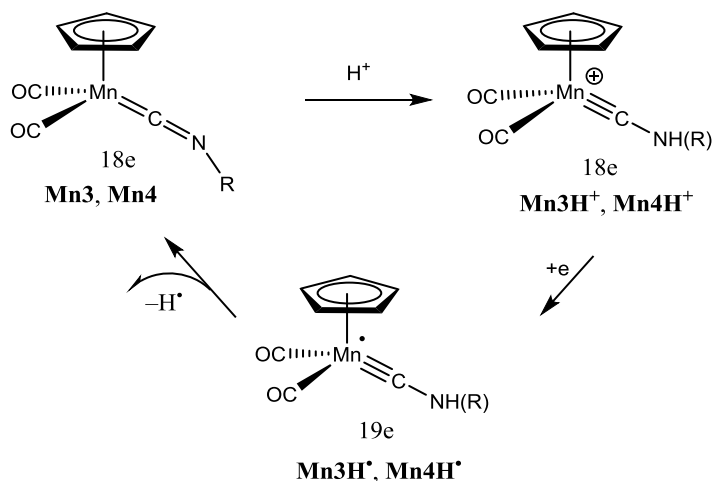
Scheme S3. Possible catalytic cycle for the electrochemical reduction of proton by complexes **Mn3** and **Mn4**.

One of the prerequisites for efficient proton reduction catalysis is the fast protonation of a catalyst on a CV time scale. The protonation of **Mn3** and **Mn4** by tetrafluoroboric acid in dichloromethane was found to occur slowly and requires a large excess of (15–20 equiv.) of the acid to be used according to the data of IR spectroscopy. Even at such a large excess, the protonation is incomplete and shifted towards starting isocyanides **Mn3** and **Mn4** (Scheme S4).

ν_{CO} 1946, 1882 cm^{-1}, ν_{CN} 2144 cm^{-1} ν_{CO} 2064, 2034 cm^{-1}

Mn3   **Mn3H$^+$**

ν_{CO} 1946, 1882 cm^{-1}, ν_{CN} 2116 cm^{-1} ν_{CO} 2060, 2010 cm^{-1}

Mn4   **Mn4H$^+$**

Scheme S4. Protonation of manganese isocyanides **Mn3** and **Mn4** by HBF$_4$·OEt$_2$ in dichloromethane.

We attempted to isolate cationic aminocarbyne complexes **Mn3H$^+$** and **Mn4H$^+$** by precipitation with petroleum ether followed by washing of the resulting precipitate with diethyl ether in order to eliminate the excess of the acid, but our attempt failed, which is likely due to the deprotonation of **Mn3H$^+$** and **Mn4H$^+$** on exposure to diethyl ether.

The incomplete protonation of **Mn3** and **Mn4** with tetrafluoroboric acid did not affect the CV, which remained unchanged upon addition of HBF$_4$·OEt$_2$. No protonated forms **Mn3H$^+$** and **Mn4H$^+$** were observed under CV conditions. Therefore, complexes **Mn3** and **Mn4** could not

exhibit catalytic activity in the electrochemical reduction of proton, which was also confirmed by CV measurements. In our opinion, their activation in this reaction requires the variation of the ligand environment of manganese atom (substitution of phosphines for CO ligand and transition from cyclopentadienyl to pentamethylcyclopentadienyl), which will be the subject of our further studies.

Electrochemical data for Mn3 and Mn4

The cyclic voltammogram of **Mn3** displays two oxidation peaks at +0.25 V (reversible peak **K**) and +1.17 V (irreversible peak **L**) (Fig. S9).
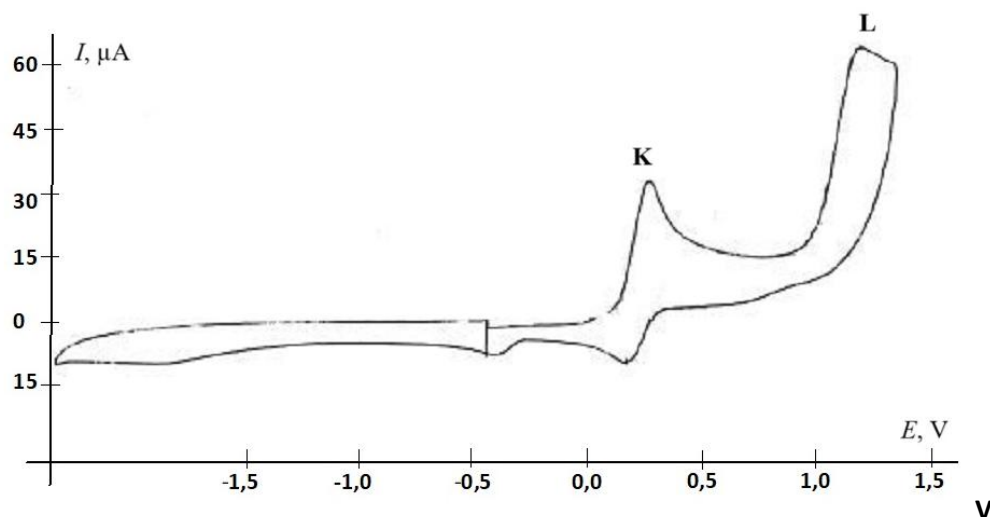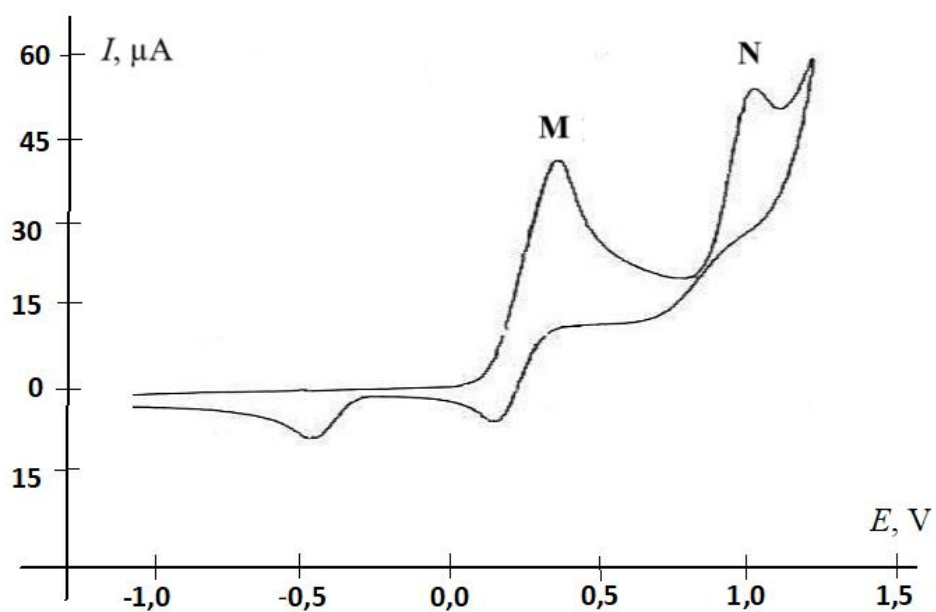

Figure S9. CV for the oxidation of $(\eta^5$-$C_5H_5)(CO)_2Mn=C=NMe$ (**Mn3**) (GC electrode, CH_2Cl_2, 0.1 M Bu_4NPF_6, $1\cdot10^{-3}$ M, 200 mV/s, potentials are given relative to Fc/Fc^+).

Figure S10 shows that the first oxidation peak **K** of **Mn3** is reversible.
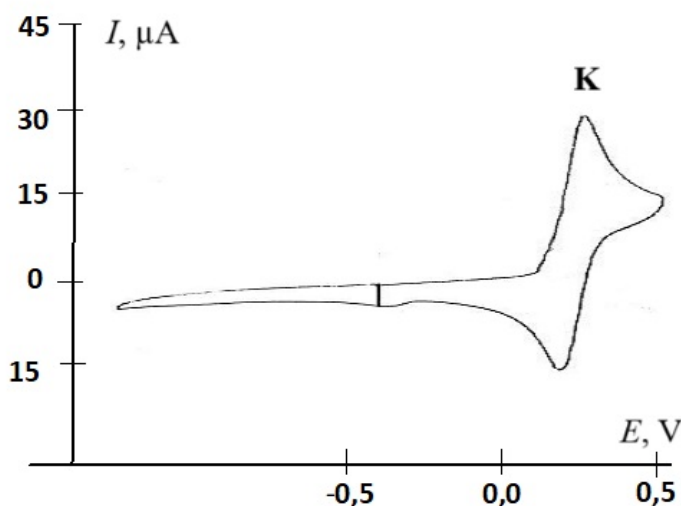
Figure S10. CV for the first oxidation of $(\eta^5$-$C_5H_5)(CO)_2Mn=C=NMe$ (**Mn3**) (GC electrode, CH_2Cl_2, 0.1 M Bu_4NPF_6, $1\cdot10^{-3}$ M, 200 mV/s, potentials are given relative to Fc/Fc^+).

The CV of $CpMn(CO)_2CN^tBu$ (**Mn4**) is similar to that observed for the manganese methylisocyanide; the only difference is the values of oxidation potentials. It displays two oxidation peaks at +0.38 V (reversible peak **M**) and +1.03 V (irreversible peak **N**) (Fig. S11).

Figure S11. CV for the oxidation (η^5-C$_5$H$_5$)(CO)$_2$Mn=C=N^{t}Bu (**Mn4**) (GC electrode, CH$_2$Cl$_2$, 0.1 M Bu$_4$NPF$_6$, $1\cdot10^{-3}$ M, 200 mV/s, potentials are given relative to Fc/Fc$^+$).

No changes in the cyclic voltammograms of **Mn3** and **Mn4** were observed upon addition of HBF$_4$·OEt$_2$ in dichloromethane.

Syntheses

Synthesis of phenylvinylidene(dicarbonyl)(η^5-pentamethylcyclopentadienyl)rhenium Cp*(CO)$_2$Re=C=C(H)Ph (Re1). A solution of Cp*Re(CO)$_3$ (810 mg, 2 mmol) in dry THF (150 mL) in a 150-mL photochemical reactor was irradiated for 1 h using a DRL-150 mercury lamp placed in a quartz water jacket upon vigorous stirring, maintaining the external dry ice–ethanol bath temperature below –20 °C. During irradiation, the solution colored in olive and IR monitoring showed that most of Cp*Re(CO)$_3$ transformed into tetrahydrofuran complex Cp*(CO)$_2$Re(THF) (v_{CO} 1894, 1822 cm^{-1}). Further irradiation did not favor an increase in the intensity of bands for Cp*(CO)$_2$Re(THF) and, therefore, irradiation was terminated. Phenylacetylene (219 µL, 203.7 mg, 2 mmol) was added dropwise. The mixture was stirred for 30 min, concentrated to a volume of about 20–30 mL, and stirred at room temperature until complete disappearance of the bands for Cp*(CO)$_2$Re(THF), which transformed into a π-alkyne intermediate Cp(CO)$_2$Re{η^2-HC≡CPh} (v_{CO} 1956, 1884 cm^{-1}). The mixture was evaporated, then dry toluene (25 mL) was added. The resulting solution was heated at 100–110 °C overnight. After 18 h of stirring, the bands for the π-alkyne complex disappeared and the new bands of complex **Re1** (v_{CO} 1982, 1914 cm^{-1}) appeared. After evaporation, the residue obtained was dissolved in a minimum amount of benzene and the resulting solution was passed through a silica gel column (10×1 cm), eluting the substance with benzene until the eluate became colorless. The eluate was evaporated to dryness and the residue obtained was washed three times with cold diethyl ether (3×10 mL). In such a manner, all impurities and starting Cp*Re(CO)$_3$ well soluble in ether were separated to give pure red-orange product **Re1**, which was dried under vacuum to produce a red-orange powder (214 mg, 25.5%) poorly soluble in hexane or diethyl ether and soluble in benzene or dichloromethane. IR (n-hexane, v/cm^{-1}): 1990 (s, CO), 1926 (s, CO). ^{1}H NMR (CDCl$_3$, 25 °C): δ 1.77 (s, 15H, Me), 4.45 (s, 1H, C=C*H*Ph), 6.93 (t, H_{para} Ph), 7.19 (dd, 2H, H_{meta} Ph), 7.29 (d, 2H, H_{ortho} Ph). ^{13}C NMR (CDCl$_3$, 25 °C): δ 10.55 (Me), 103.02 (=*C*HPh), 118.50 (C_{ortho} Ph), 125.5 (C_{para} Ph), 128.8 (C_{meta} Ph), 130.7 (C_{ipso} Ph), 124.75 (C_5Me$_5$), 202.50 (*C*O), 332 (Re=*C*). MS (EI), m/z: 480 (M), 452 (M–1CO), 424 (M–2CO), 409 (M–2CO–1CH$_3$).

Synthesis of phenylethynyl(carbonyl)(triphenylphosphine)(η^5-cyclopentadienyl)iron Cp(CO)(PPh$_3$)Fe–C≡CPh (Fe1). A solution of iron acetylide Cp(CO)$_2$Fe–C≡CPh (278 mg, 1 mmol) and PPh$_3$ (288 mg, 1.15 mmol) in THF (150 mL) placed in a 150-mL photochemical reactor was irradiated for 1 h upon vigorous stirring using a DRL-150 mercury lamp placed in a quartz water jacket, maintaining the external dry ice–ethanol bath temperature below +10 °C. The solvent was evaporated under vacuum and the residue obtained was purified by flash chromatography on silica gel using benzene as an eluent. The resulting brown fraction was evaporated to dryness and the residue obtained was recrystallized from hexane to yield 308 mg (60%) of complex **Fe1**. IR (n-hexane, v/cm^{-1}): 2095 (w, C≡C), 1945 (m, CO). ^{1}H NMR (400 MHz, C$_6$D$_6$, 25 °C): δ 4.26 (d, $^3J_{HP}$ = 1.12 Hz, 5H, Cp), 6.90–6.96 (tt, 1H, *Ph*), 6.97–7.04 (m, 9H, *Ph*), 7.05–7.10 (tt, 2H, P*Ph*), 7.27–7.32 (dm, 2H, P*Ph*), 7.75–7.84 (m, 6H, *m-H* PPh). ^{13}C NMR (101 MHz, C$_6$D$_6$, 25 °C): δ 84.35 (broad s, Cp), 106.06 (d, $^3J_{CP}$ = 42 Hz, Fe*C*≡), 120.55 (d, $^3J_{CP}$ = 2.7 Hz, ≡*C*Ph), 124.14 (s, Ph), 127.58, 127.82, 127.87 (all s, P*Ph*), 129.73 (d, 2.45 Hz, P*Ph*), 130.28 (d, J_{CP} = 1.29 Hz, P*Ph*), 131.14 (s, Ph), 133.58 (d, J_{CP} = 9.6 Hz, P*Ph*), 136.72 (d, $^1J_{CP}$ = 43.98 Hz, P*Ph*), 220.24 (d, $^2J_{CP}$ = 30.3 Hz, Fe*C*O). ^{31}P NMR (162 MHz, C$_6$D$_6$, 25 °C): δ 75.79 (Fe*P*Ph$_3$).

Earlier this complex was obtained by Green and Mole [S7] in good yield (a specific value was not given), heating iron dicarbonyl phenylethynyl complex $Cp(CO)_2Fe–C≡CPh$ at 160 °C in the presence of PPh_3. Its protonated form $[Cp(CO)(PPh_3)Fe^+=C=C(H)Ph]BF_4^-$ (**Fe1H$^+$**) was described by Davison [S8].

Dicarbonyl phenylethynyl complex $Cp(CO)_2Fe–C≡CPh$ was synthesized by the CuI-catalyzed reaction of cyclopentadienyl(dicarbonyl)iron chloride $Cp(CO)_2FeCl$ with phenylacetylene in the presence of triethylamine [S9]. Starting $Cp(CO)_2FeCl$ was synthesized from cyclopentadienyliron dicarbonyl dimer $[CpFe(CO)_2]_2$ upon its visible-light irradiation in chloroform [S10].

Synthesis of methylisocyanide(dicarbonyl)(η^5-cyclopentadienyl)manganese $Cp(CO)_2Mn=C=NMe$ (Mn3). A solution of cymantrene (1.02 g, 5 mmol) in dry THF (150 mL) placed in a 150-mL photochemical reactor was irradiated for 1 h upon vigorous stirring using a DRL-150 mercury lamp placed in a quartz water jacket, maintaining the external dry ice–ethanol bath temperature below –20 °C. During irradiation, the solution became a ruby-colored and its IR spectrum displayed v_{CO} bands at 1924, 1844 cm^{-1} corresponding to tetrahydrofuran complex $Cp(CO)_2Mn(THF)$, with no bands for starting cymantrene being observed. Methylisocyanide (550 µL, 410.3 mg, d_{25} = 0.746 g/mL, 10 mmol) was added, and the mixture was stirred for 2.5 h. During this time, the mixture turned to light-yellow. The IR spectrum displayed bands for title product **Mn3** (v_{CN} 2142, v_{CO} 1948, 1888 cm^{-1}). The solvent was evaporated under vacuum, and the residue obtained was purified by chromatography on silica gel (20×3 cm). The organic impurities and unreacted cymantrene were eluted first with hexane and then with a petroleum ether–benzene mixture (1:1). The target isocyanide complex was eluted with pure benzene. The eluate was evaporated, and the residue was recrystallized from n-hexane to yield 760 mg (70%) of **Mn3** as a yellow crystalline powder. IR (n-hexane, v/cm^{-1}): 2130 (m, C≡N), 1958 (s, CO), 1908 (s, CO). MS (EI), m/z: 217 (M), 161 (M–2CO), 120 (M–2CO–CNMe), 55 (Mn$^+$). ^{1}H NMR (C_6D_6, 600.13 MHz, 25 °C): δ 2.15 (br. s, 3H, NCH_3), 4.23 (s, 5H, C_5H_5). ^{13}C NMR (C_6D_6, 150.90 MHz, 25 °C): δ 29.13 (NCH_3), 81.74 (C_5H_5), 177.33 (Mn=C=N), 230.86 (MnCO).

Earlier two methods for the preparation of **Mn3** were described. In the first method [S11], a solution of cymantrene and methylisocyanide in THF was UV irradiated to give the target product in 90% yield. In the second method [S12], the carbonyl ligand was replaced with methylisocyanide upon heating in toluene in the presence of PdO catalyst, but the yield was only 5%. Since it is known that all three CO ligands could be replaced with three isocyanide molecules, we slightly modified the photochemical procedure [S11] and carried out a stepwise substitution of THF for CO and then THF for methylisocyanide as described above.

Synthesis of *tert*-butylisocyanide(dicarbonyl)(η^5-cyclopentadienyl)manganese $Cp(CO)_2Mn=C=N^tBu$ (Mn4). A solution of cymantrene (1.0 g, 4.9 mmol) in dry THF (150 mL) placed in a 150-mL photochemical reactor was irradiated for 1 h upon vigorous stirring using a DRL-150 mercury lamp placed in a quartz water jacket, maintaining the external dry ice–ethanol bath temperature below –20 °C. During irradiation, the solution became a ruby-colored and its IR spectrum displayed v_{CO} bands at 1924, 1844 cm^{-1} corresponding to tetrahydrofuran complex $Cp(CO)_2Mn(THF)$, with no bands for starting cymantrene being observed. *tert*-Butylisocyanide (410 µL, 301 mg, d_{25} = 0.735 g/mL, 3.6 mmol) was added, and the mixture was stirred for 2.5 h. During this time, the mixture turned light-yellow. The IR spectrum displayed bands for title product **Mn4** (v_{CN} 2110, v_{CO} 1946, 1890 cm^{-1}). The solvent was evaporated under vacuum, and the residue obtained was dissolved in a minimum amount of benzene and purified by

chromatography on silica gel (20×3 cm). The organic impurities and unreacted cymantrene were eluted first with hexane and then with a petroleum ether–benzene mixture (1:1). The fraction with the target isocyanide complex was eluted with pure benzene. The eluate was evaporated and the residue was recrystallized from n-hexane to yield 730 mg (78.3% based on ^{t}BuNC) of **Mn4** as a yellow crystalline powder. IR (n-hexane, v/cm^{-1}): 2070 (m, C≡N), 1956 (s, CO), 1910 (s, CO). MS (EI), m/z: 259 (M), 203 (M–2CO), 147 (M–2CO–C_4H_8), 120 (M–2CO–CN^{t}Bu), 55 (M–2CO–CN^{t}Bu–C_5H_5). ^{1}H NMR (C_6D_6, 600.13 MHz, 25 °C): δ 0.94 (br. s, 9H, CH_3), 4.24 (s, 5H, C_5H_5). ^{13}C NMR (C_6D_6, 150.90 MHz, 25 °C): δ 30.73 (CH_3), 57.06 (NC(CH$_3$)$_3$), 81.90 (C_5H_5), 179.86 (Mn=C=N), 230.65 (MnCO).

In the literature, there are no reports on the photochemical preparation of **Mn4**, but manganese *tert*-butylisocyanide **Mn4** has been obtained earlier [S12] in 60% yield by the palladium oxide-catalyzed reaction upon heating in toluene.

References

S1. T. Agarwal, S. Kaur-Ghumaan, *Coord. Chem. Rev.*, **2019**, *397*, 188–219. DOI: 10.1016/j.ccr.2019.06.019

S2. R. E. Adams, T. A. Grusenmeyer, A. L. Griffith, R. H. Schmehl, *Coord. Chem. Rev.*, **2018**, *362*, 44–53. DOI: 10.1016/j.ccr.2018.02.014

S3. I. O. Shotonwa, B. Kpomah, B. M. Durodola, A. O. Adesoji, W. Plass, Sh. Adewuyi, *J. Electroanal. Chem.*, **2024**, *973*, 118664. DOI: 10.1016/j.jelechem.2024.118664

S4. E. Portenkirchner, K. Oppelt, D. A. M. Egbe, G. Knör, N. S. Sariçiftçi, *Nanomater. Energy*, **2013**, *2*, 134–147. DOI: 10.1680/nme.13.00004

S5. B. H. Solis, A. G. Maher, D. K. Dogutan, D. G. Nocera, S. Hammes-Schiffer, *PNAS*, **2016**, *113*, 485–492. DOI: 10.1073/pnas.1521834112

S6. J. L. Dempsey, *PNAS*, **2016**, *113*, 478–479. DOI: 10.1073/pnas.1522759113

S7. M. L. H. Green, T. Mole, *J. Organomet. Chem.*, **1968**, *12*, 404–406. DOI: 10.1016/S0022-328X(00)93865-8

S8. A. Davison, J. P. Solar, *J. Organomet. Chem.*, **1978**, *155*, C8–C12. DOI: 10.1016/S0022-328X(00)90432-7

S9. M. I. Bruce, M. G. Humphrey, J. G. Matisons, S. K. Roy, A. G. Swincer, *Aust. J. Chem.*, **1984**, *37*, 1955–1961. DOI: 10.1071/CH9841955

S10. S. Komiya, M. Hurano, in: *Synthesis of Organometallic Compounds. A Practical Guide*, S. Komiya (Ed.), Wiley, **1997**, pp. 177–178.

S11. P. M. Treichel, H. J. Mueh, *Inorg. Chim. Acta.*, **1977**, *22*, 265–268. DOI: 10.1016/S0020-1693(00)90929-0

S12. G. W. Harris, J. C. A. Boeyens, N. J. Couville, *J. Organomet. Chem.*, **1983**, *255*, 87–94. DOI: 10.1016/0022-328X(83)80176-4